Stability in flexible torus-like crystals effected by dislocations and twist

Bohan Cao* and Yao Li†
School of Physics, Nankai University, Tianjin, 300071, China

We study the properties in flexible crystalline membranes of torus-like topology effected by dislocations and twist. Using computational modeling, we obtain the trend of properties under different twists and dislocations. We divide the crystal into three categories based on the location of dislocation when stable. Our findings reveal a design space for controllable torus-like geometries.

INTRODUCTION

With the rise of research on materials such as carbon nanotubes[1], the special properties of two-dimensional materials are receiving increasing attention. Two dimensional materials refer to materials in which electrons can only move freely in two mesoscopic dimensions. Membranes are two dimensional objects embedded in three dimensional space. Flexible torus-like crystal is a kind of two-dimensional crystal with closure constraint, which brings new properties. The torus material such as $BaTiO_3$ was shown to have special electromagnetic properties.[2] Andrei Zakharov studied shape multistability in freestanding tubular crystals for two kinds of achiral tubular crystals.[3] We apply their methods to flexible torus-like crystals.

We consider the effects of twists and dislocations on the model. We consider the effects of single dislocation pair, which is the simplest defects which can be constructed in finite steps from perfect crystal. Only gilde types in dislocations is considerated here. We consider different twist and phases as Fanlong Meng did in the paper study phase diagram under of an inflated soft tube under twist[4]. We show the shape transformation under different twist.

The molecular dynamics simulation[5] is performed to minimize energy under NVT ensemble. All physical quantities are measured in reduced units. The microscale configurations are visualized using the Ovito software[6]. The Kokkos[7] library is used to support parallel computing.

COMPUTATIONAL MODEL

For a tubular crystal, parastichies are the helical paths around tube, only allowed to have a discrete set of possible angles with the tube axis. The number of distinct parastichies defines a pair of integer parastichy numbers, which index the possible crystalline tessellations of the cylinder.[8] For a torus-like crystal, it is needed to use additional parameters to describe the structure since there are only a limited number of particles on the tube and twist will take effect.

As shown in figure 1(a), its difficult to disdiguish layers on chiral tubes since there isn't any parastichy perpendicular to the tube axis. In the achiral case shown in figure 1(b), one layer consist of $m(n)$ particles and number of layers l can be used as an additional parameter. We use another additional parameter t called twist degree, which means the number of particles shifted when ends meet. For example, when rolled into a torus, the particle A would coincide with particle C naturally since AC is parallel to the tube axis, while it is forced to coincide with B or D. In the latter cases, the corresponding twist degree is 1 and -1.

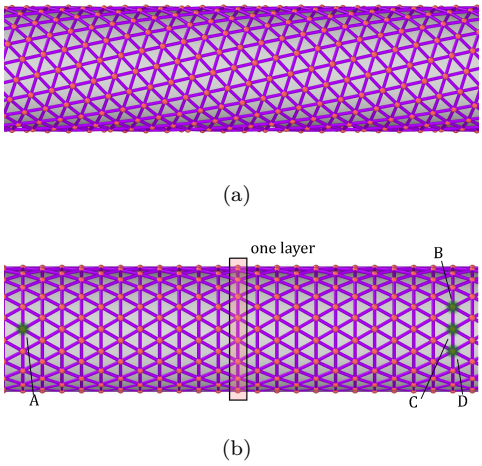

(a)

(b)

FIG. 1. (a) Chial ($m = 20$, $n = 14$) and (b) achiral ($m = n = 17$) tube structures. For the convenience of observation, the particles on the back are obscured.

We model the crystal as a network of harmonic spring bonds with a cuverature energy at each node proportional to the sum of squared principal curvatures. The coefficient of cuverature energy called bending rigidity κ. The potential energy is

$$F = \frac{\epsilon}{2}\sum_{\text{bonds}}(l_{ij} - l_0)^2 + \frac{\kappa}{2}\sum_{\text{nodes}}(4H_i^2 - 2K_i)A_i, \quad (1)$$

where l_0 represents the original length of each bond, the observed area A_i around a node is one third of the total area, H_i is discrete mean curvature and K_i is discrete Gaussian curvature, which can be evaluated by

$$K_i = \frac{2\pi - \sum \rho_j}{A_i}, H_i = \frac{\|\sum_j((\boldsymbol{x}_i - \boldsymbol{x}_j)(\cot\varphi_{ij}^1 + \cot\varphi_{ij}^2))\|}{4A_i}. \quad (2)$$

Let $l_0 = 1$ and the Young's modulus of a membrane $Y = 2\epsilon/\sqrt{3} = 1$ in reduced unit system, then the elastic coefficient can be reduced to $\epsilon = \sqrt{3}/2$, and the reduced bending rigidity is $\kappa^* = \kappa/\epsilon l_0^2$. The reduced potential energy $U^* = U/\epsilon l_0^2$ can be written as

$$U^* = \frac{\sqrt{3}}{4}\sum_{\text{bonds}}(l_{ij}^* - 1)^2 + \frac{\kappa^*}{2}\sum_{\text{nodes}}(4H_i^{*2} - 2K_i^*)A_i^*. \quad (3)$$

The overdamped Langevin equation is used to describe the evolutionary behavior of the system. Let damping coefficient $\gamma = 1$ in reduced system. Then the reduced temperature is $T^* = k_B T/\epsilon l_0^2$, and the reduced time is $t^* = \epsilon t/\gamma$. So the overdamped Langevin equation can be written

$$\frac{\partial \boldsymbol{X}^*}{\partial t^*} = -\frac{\partial U^*}{\partial \boldsymbol{X}^*} + \sqrt{\frac{2T^*}{\mathrm{d}t^*}}\eta, \quad (4)$$

where η is a vector with uniform angular distribution and uniform radial distribution in $(0, 1)$. The central limit theorem ensures that this is equivalent to a Gaussian distribution. The asterisk on physical quantities will be omitted in the following text.

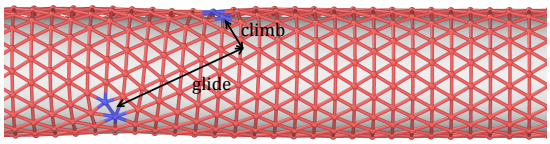

FIG. 2. Dislocations ($m = n = 17$)

As shown in figure 2, dislocation pair is a pair of disloaction with opposite Burgers vector, and can be constructed by glide and climb. The distance between two dislocations can be represented by number of glide steps g and climb steps c as[3]

$$x = \frac{\sqrt{3}}{2}c\sin\theta + g\cos\theta, y = -\frac{\sqrt{3}}{2}c\cos\theta + g\sin\theta. \quad (5)$$

In this paper, only glides perpendicular to axis is considerated.

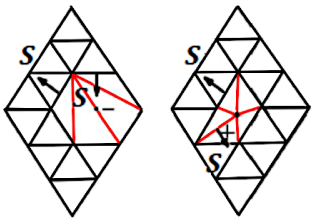

FIG. 3. Transitions of climbs. Remove atom (left) and add atom (right).

Defects are obtained through transition of a perfect crystal. Glides are obtained by $T1$ transition, while climbs are obtained by transitions shown in figure 3.

AFFECTED PARAMETERS

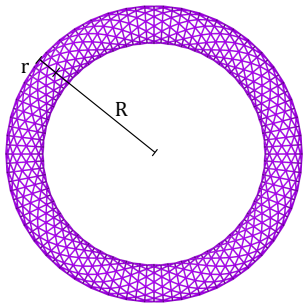

FIG. 4. Torus $m = n = 13, l = 100, t = 0$

As shown in figure 4, the outer radius of torus is R, while the inner radius is r. The outer radius stretching factor is defined as R/R_0, where $R_0 = \sqrt{3}l/4\pi$. The inner radius stretching factor is defined as r/r_0, where $r_0 = m/2\pi$.

Due to the competition between curvature energy and elastic energy, the cross-section of the torus appears elliptical. Since the compression degree of the inner mesh and the stretching degree of the outer mesh are directly proportional to the distance between the inner and outer mesh, the inner and outer layers tend to approach each other. So the major axis of the cross-section ellipse is perpendicular to the plane torus located. We calculated the eccentricity by

$$e = \frac{\sqrt{a^2 - b^2}}{a}, \quad (6)$$

where a, b are the distance between the farthest / nearest particles and the average center respectively.

Twist angle is $\Phi = 2t\pi/m$, the torque T then can be defined as

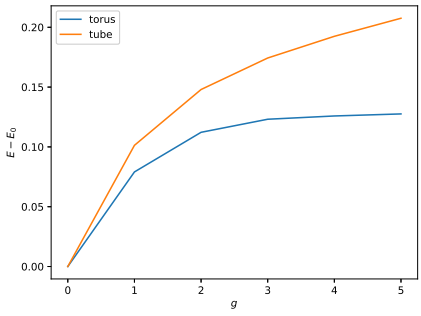

FIG. 5. Energy under different glide. g is glide, $E - E_0$ is energy increment from perfect crystal. $m = n = 13, l = 100, t = 0, \kappa = 0.1$

$$T = \frac{\partial U}{\partial \Phi}. \tag{7}$$

The twist parameter is $\phi = \Phi r / 2\pi R$ [4].

As shown in figure 5, the shape of torus can slow down the change of energy while glide changes. That's may because defects can cause bending, which can adapt to the bending of torus itself.

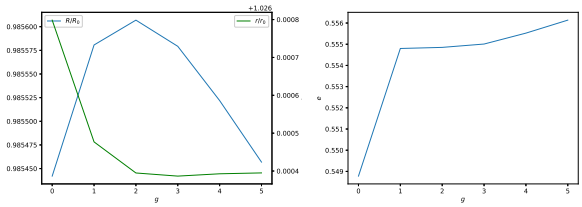

FIG. 6. Stretching degree of inner and outer radius and eccentricity. $m = n = 13, l = 100, t = 0, \kappa = 0.1$

As shown in figure 6, the shape of torus can increase inner raduis ($r/r_0 > 1$) and decrease outer raduis ($R/R_0 < 1$). Gilde would change the stretching degree to a very small extent and increase eccentricity.

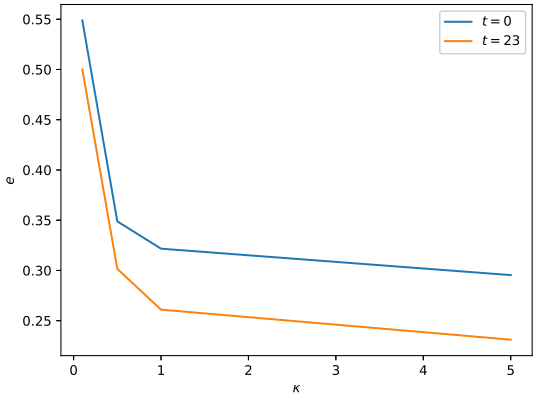

FIG. 7. Eccentricity under different reduced bending rigidity. $m = n = 13, l = 100, g = 0$

As shown in figure 7, eccentricity is mostly decided by reduced bending rigidity, and less affected by t and g. The higher reduced bending rigidity, the lower eccentricity.

As shown in figure 8, the torque increases as twists increases, which means the torus will become harder and harder. Stretching degree of inner radius decreases as twists increases, while stretching degree of outer radius increases as twists increases. This means that twist degree can offset the effect of inner and outer radius changes caused by the shape of torus.

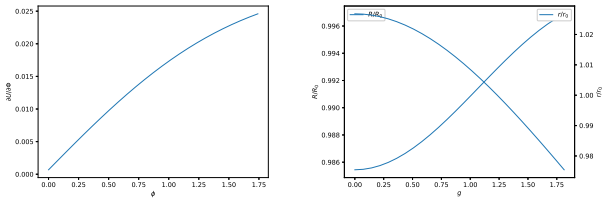

FIG. 8. Torque and Stretching degree of inner and outer radius under different twists. $m = n = 13, l = 100, \kappa = 0.1, g = 0$

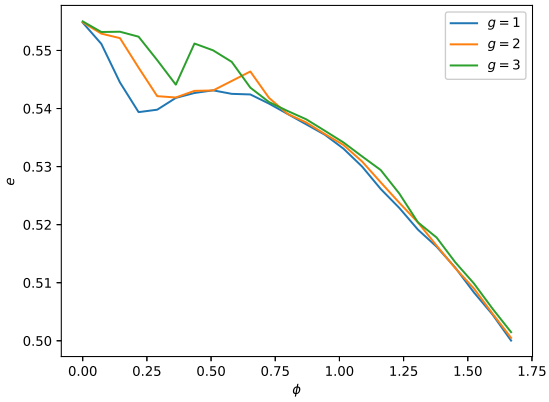

FIG. 9. Eccentricity under different twists. $m = n = 13, l = 100, \kappa = 0.1$

As shown in figure 9, the eccentricity decreases as t increases. However, this is not completely monotonous, since there are points increased in local intervals. We found these points are near the phase transition point, and may be caused by phase transition.

PHASE DIAGRAM

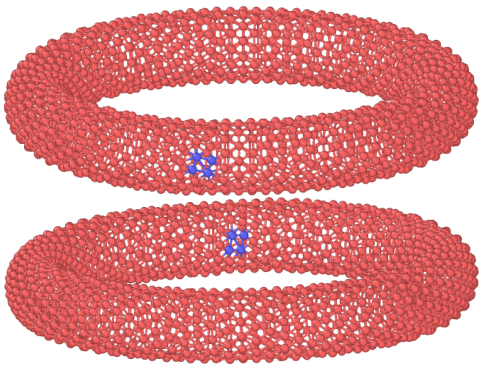

FIG. 10. Two phases. (up) Phase of outer dislocations. (down) Phase of inner dislocations.

As mentioned earlier, twist can cause parameter changes and lead to phase transitions. Since the variation of parameters is continuous, it is a second-order phase transition. In the structure of torus, this phase transition is shown as defect position flipping.

As shown in figure 10, when the t is small, the dislocations is at outer surface, with t increases, the dislocations move to inner surface suddenly at a certain point. This is first phase transition and is a second-order phase transition. At a higher t, the torus won't exsit stable and will collapse into a line or other structure such as in figure 11, which don't have any continuous parameters and is a first-order phase transition.

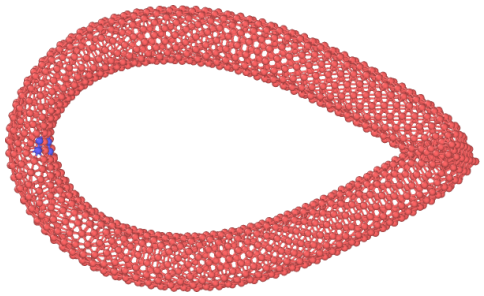

FIG. 11. One kind of collapsed structure. $m = m = 13, l = 100, g = 2, t = 25, \kappa = 0.1$

As shown in figure 12, the phase can be divided into three.

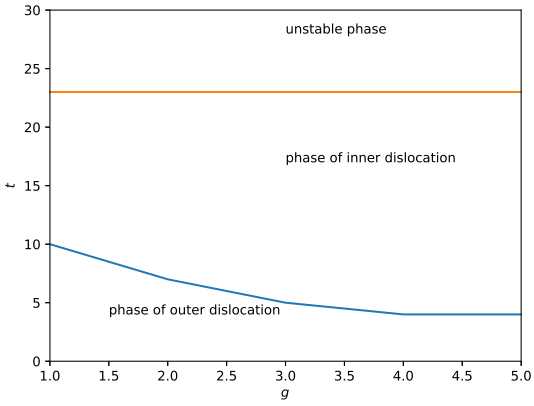

FIG. 12. Phase of torus. $m = m = 13, l = 100, \kappa = 0.1$

DISCUSSION

Our findings can be used to study micro torus-like biomaterial. Futher study could focus on the origin of the different phases.

The universally applicable method of torus discription haven't be found yet. Additional parameters need to be proposed to study any kinds of torus including chial torus, which may bring new propeties.

ACKNOWLEDGMENT

This work was supported by the Pilot Scheme of Talent Training in Basic Sciences (Boling Class of Physics, Nankai University), Ministry of Education.

This work was supported by the National Science Fund for Talent Training in the Basic Sciences (No. J1103208).

* 2110313@mail.nankai.edu.cn
† liyao@nankai.edu.cn

[1] A. Thess, R. Lee, P. Nikolaev, *et al.*, Crystalline ropes of metallic carbon nanotubes, science **273**, 483 (1996).
[2] F. Xia, J. Liu, D. Gu, P. Zhao, J. Zhang, and R. Che, Microwave absorption enhancement and electron microscopy characterization of batio3 nano-torus, Nanoscale **3**, 3860 (2011).
[3] A. Zakharov and D. A. Beller, Shape multistability in flexible tubular crystals through interactions of mobile dislocations, Proceedings of the National Academy of Sciences **119**, e2115423119 (2022).
[4] F. Meng, J. Z. Y. Chen, M. Doi, and Z. Ouyang, enThe phase diagram and radial collapse of an inflated soft tube under twist, Soft Matter **11**, 7046 (2015).
[5] D. Frenkel and B. Smit, *Understanding Molecular Simulation: From Algorithms to Applications* (Elsevier, 2002) pp. 23–105.
[6] A. Stukowski, Visualization and analysis of atomistic simulation data with ovito-the open visualization tool, Modelling and Simulation in Materials Science and Engineering **18**, 015012 (2010).
[7] C. R. Trott, D. Lebrun-Grandie, D. Arndt, *et al.*, Kokkos 3: Programming Model Extensions for the Exascale Era, IEEE Transactions on Parallel and Distributed Systems **33**, 805 (2022).
[8] L. Fu, W. Steinhardt, H. Zhao, J. E. S. Socolar, and P. Charbonneau, Hard sphere packings within cylinders, Soft Matter **12**, 2505 (2016).